



HAL
open science

Bridging the Li-Carter's gap: a locally coherent mortality forecast approach

Quentin Guibert, Stéphane Loisel, Olivier Lopez, Pierrick Piette

► **To cite this version:**

Quentin Guibert, Stéphane Loisel, Olivier Lopez, Pierrick Piette. Bridging the Li-Carter's gap: a locally coherent mortality forecast approach. 2020. hal-02472777

HAL Id: hal-02472777

<https://hal.science/hal-02472777>

Preprint submitted on 10 Feb 2020

HAL is a multi-disciplinary open access archive for the deposit and dissemination of scientific research documents, whether they are published or not. The documents may come from teaching and research institutions in France or abroad, or from public or private research centers.

L'archive ouverte pluridisciplinaire **HAL**, est destinée au dépôt et à la diffusion de documents scientifiques de niveau recherche, publiés ou non, émanant des établissements d'enseignement et de recherche français ou étrangers, des laboratoires publics ou privés.

Bridging the Li-Carter's gap: a locally coherent mortality forecast approach

Quentin Guibert^{*1,2,5}, Stéphane Loisel^{†1}, Olivier Lopez^{‡3}, and Pierrick Piette^{§1,4}

¹Univ Lyon, Université Claude Bernard Lyon 1, Institut de Science Financière et d'Assurances (ISFA),
Laboratoire SAF EA2429, F-69366, Lyon, France

²Ceremade, UMR 7534, Université Paris-Dauphine, PSL Research University, 75016 Paris, France

³Sorbonne Université, CNRS UMR 8001, Laboratoire de Probabilités Statistique et Modélisation, LPSM, 4
place Jussieu, F-75005 Paris, France.

⁴Seyna, 58 rue de la Victoire, 75009 Paris, France

⁵Prim'Act, 42 avenue de la Grande Armée, 75017 Paris, France

February 7, 2020

Abstract

Countries with common features in terms of social, economic and health systems generally have mortality trends which evolve in a similar manner. Drawing on this, many multi-population models are built on a coherence assumption which inhibits the divergence of mortality rates between two populations, or more, on the long run. However, this assumption may prove to be too strong in a general context, especially when it is imposed to a large collection of countries. We also note that the coherence hypothesis significantly reduces the spectrum of achievable mortality dispersion forecasts for a collection of populations when comparing to the historical observations. This may distort the longevity risk assessment of an insurer. In this paper, we propose a new model to forecast multiple populations assuming that the long-run coherent principle is verified by subgroups of countries that we call the "locally coherence" property. Thus, our specification is built on a trade-off between the Lee-Carter's diversification and Li-Lee's concentration features and allows to fit the model to a large number of populations simultaneously. A penalized vector autoregressive (VAR) model, based on the elastic-net regularization, is considered for modeling the dynamics of common trends between subgroups. Furthermore, we apply our methodology on 32 European populations mortality data and discuss the behavior of our model in terms of simulated mortality dispersion. Within the Solvency II directive, we quantify the impact on the longevity risk solvency capital requirement of an insurer for a simplified pension product. Finally, we extend our model by allowing populations to switch from one coherence group to another. We then analyze its incidence on longevity hedges basis risk assessment.

JEL Classification: C18, C32, C53, J11.

Keywords: Coherent mortality forecasting; Multi-population; Basis risk; Vector Autoregression; Elastic-Net.

*Email: guibert@ceremade.dauphine.fr.

†Email: stephane.loisel@univ-lyon1.fr.

‡Email: olivier.lopez0@upmc.fr.

§Email: pierrick.piette@gmail.com.

1 Introduction

Around the world, the life expectancy of many countries has significantly risen over the past decades. This general augmentation implicitly suggests that common drivers are shared between populations such as lifestyle factors, the level of socioeconomic inequalities or the quality of the health system. However, this improvement is not equally shared among all groups of populations, precisely because the driving features are heterogeneous at an individual level. The links and differences between groups are important to understand for demographic and actuarial studies, since they may cause issues in managing social security system, pension funds or in defining longevity risk hedging solution. This explains the growing interest in mortality forecasting of multiple populations, especially to understand the effect of sub-groups on an overall population (Danesi et al., 2015; Bergeron-Boucher et al., 2018; Cairns et al., 2019) or to enhance the projections robustness for populations with not well-known trends, see e.g. Li et al. (2018).

Since the introduction of the augmented common factor approach by Li and Lee (2005), many multi-population models have been developed. Most of them are extensions of the Lee and Carter (1992) model or the CDB models (Cairns et al., 2006), and rely on a so-called coherence principle, see Villegas et al. (2017) for a review. This concept, introduced by Li and Lee (2005), consists in imposing that the mortality rates of two populations (or more) do not diverge in the long run. In such a specification, common age and period effects are estimated for a group of mortality data, the population specific trend being therefore modeled via mean-reverting process. This principle is also introduced in the so-called GRAVITY model (Dowd et al., 2011) or in the Common Age Effect (CAE) model (Kleinow, 2015; Enchev et al., 2017). Although this assumption may be relevant for close populations, Li et al. (2017) have pointed out that it is often only suitable for specific populations and over limited time windows. Hence, this approach is more likely to become unsatisfactory when it is applied to a large collection of populations. Furthermore, by inhibiting the divergence between populations, an irrelevant use of the mortality convergence principle may thereby distort the projections spectrum of mortality dispersion among the populations. In that context, extending the current mortality forecasting models for a large number of populations is challenging as it involves to cluster together similar countries and separately forecasting those with diverging mortality dynamics, as noted by Richman and Wuthrich (2018).

Motivated by the need of applying stochastic mortality models to a large collection of populations, our aim in this paper is to find a trade-off between the full coherence principle between populations and the noncoherence situation where single stochastic mortality models are considered independently. These two situations can be considered as border cases of the inter-group dependence possibilities, and are both undesirable, in a general context, for life insurers which are assisted by stochastic mortality multi-population models in their longevity risk solvency capital assessment. Indeed, a fully coherent model can overestimate the capital requirement through the concentration between the populations it imposes, whereas the use of independent single-population models may induce an underestimation of this capital. Note also that an inappropriate use of coherent mortality model for populations with heterogeneous mortality profiles or vice-versa can significantly affect the effectiveness of reinsurance management strategies, see e.g. Yang et al. (2019). Similar problem appears also for the pricing and the hedging of longevity risk transfer solutions where an accurate risk assessment is required, especially for the corresponding basis risk.

To overcome this issue, Li et al. (2017) introduce the concept of semicoherence which contains the mortality differentials into a tolerance corridor. In other words, the two population mortality dynamics can diverge over certain periods of time, but not permanently. Their semicoherent mortality projection is based on a threshold vector autoregressive process, which can be seen as a

vector autoregressive (VAR) model characterized by a parameter set and autoregressive order which change according to the time series regime. Zhou et al. (2019) recently improve this approach by introducing a threshold vector error correction model and taking into account long-term equilibrium between time series. However, these models are developed for only two populations and their VAR structure contained many parameters, which is a serious limitation in the large-scale mortality forecasting framework.

In this paper, we propose an alternative approach, named "local coherence", which allows us to model simultaneously a large collection of populations by assuming the mortality coherence principle is satisfied for several subgroups of populations. Although our approach is mainly based on existing models, such as the Lee-Carter or the Li-Lee models, it intends to gain in flexibility by offering a trade-off between diverging mortality forecasts, obtained with a single stochastic mortality model, and fully coherence forecasts. In that way, our goal is similar to the Li et al. (2017) semicoherence one, i.e. offering a compromise between the fully coherence and the independence situations, even if the approach differs. Notably, in our case the size of the populations collection can be large and the proposed model includes the two border cases.

Within a locally coherent group, the dynamics of the mortality is based on a Li and Lee (2005) model. To capture both long-term relationships and short-term interactions between groups, a VAR process models the improvements in the common mortality trends of each group. A similar specification for a small group of populations is proposed by several authors in the literature, see Zhou et al. (2014), Kleinow (2015), and Enchev et al. (2017) among others. However, a VAR model may suffer of over-fitting issue when the size of the group increases, since historical series are relatively short and strongly correlated. For our large-scale general context, we then use a VAR-ENET approach. Based on an elastic-net regularization technique, this VAR estimation is relevant with high dimensional time series and offers good in-sample and out-of-sample performances in a mortality forecasting framework (Guibert et al., 2019).

For illustrative purpose, we estimate our locally coherent model on a collection of 16 European countries, by distinguishing the gender. We propose two approaches to cluster these populations in coherent groups, regarding to the historical mortality rates data or expert judgments. Our results highlight a better control of the mortality rates dispersion forecasting among the populations. In addition, we show the importance of having an accurate level of variability when considering the solvency capital requirement of an European life insurer exposed to longevity risks from multiple populations.

Furthermore, we extend our model by allowing the populations to switch dynamically from one group of coherence to another. Thus, the coherence may be specified locally not only in the spatial dimension, i.e. according to the populations, but also in the temporal dimension. Such switches can be caused by changes in socio-economic features driving the mortality dynamics. We underpin the importance this extension by analyzing the impact of a specific switch on a Longevity Divergence Index Value, similar to the one that the Kortis bond is based on.

The remainder of this paper is organized as follows. In Section 2, we recall the usual Lee-Carter and Li-Lee models and show the mortality dispersion forecasting issue. Section 3 introduces our locally coherent model and shows how it fills the gap between a fully coherent and an independent situations. We also present the VAR-ENET estimation method retained in the paper. Section 4 presents two clustering approaches for identifying coherent groups: one based on expert judgments and a data-driven approach. The results obtained on the groups composed of 32 European populations is discussed, and we demonstrate the interest for the risk-based capital requirement of a life insurer in presence of multi-population exposures. Section 5 extends our model to a dynamic

local coherence, and illustrates its impact on a basis risk assessment example. Finally, Section 6 concludes the paper and gives several improvements for future researches.

2 The mortality dispersion issue

2.1 Notation

As noted in the Section 1, a large range of models have been developed for mortality modeling and forecasting within the multi-population framework. In this paper, we do not limit our study to the specific two-population context: we consider a more general scope of a collection \mathcal{I} of populations, where its cardinal $I \geq 2$ is potentially high. Furthermore, we note \mathcal{X} and \mathcal{T} the collections of integer ages and calendar years respectively.

For $(i, x, t) \in \mathcal{I} \times \mathcal{X} \times \mathcal{T}$, we note $D_{x,t}^{(i)}$ the number of people in the i -th population who die in year t and aged x at their last birthday. The so-called "exposure to risk", noted $E_{x,t}^{(i)}$, represents the amount of *person years* lived by people of population i aged $[x, x + 1)$ in year $[t, t + 1)$. Thus, the central death rate $m_{x,t}^{(i)}$ is given by

$$m_{x,t}^{(i)} = \frac{D_{x,t}^{(i)}}{E_{x,t}^{(i)}}. \quad (2.1)$$

In the two populations framework, the coherence can be analyzed by focusing on the difference of log-mortality rates at a specific age x , which we note $\delta_{x,t} = \ln m_{x,t}^{(1)} - \ln m_{x,t}^{(2)}$. The coherence hypothesis specifies that for all $x \in \mathcal{X}$, the series $(\delta_{x,t})_t$ do not diverge. We extend this measure to the general multiple populations case where I is potentially important. Thus, for an age and time (x, t) , and a collection \mathcal{I} of populations, we define $\delta_{x,t}^{\mathcal{I}}$ the dispersion of mortality rates

$$\delta_{x,t}^{\mathcal{I}} = \sqrt{\frac{1}{I-1} \sum_{i \in \mathcal{I}} \left(\ln m_{x,t}^{(i)} - \overline{\ln m_{x,t}} \right)^2}, \quad (2.2)$$

where $\overline{\ln m_{x,t}} = \frac{1}{I} \sum_{i \in \mathcal{I}} \ln m_{x,t}^{(i)}$ is the mean of log mortality rates over the collection \mathcal{I} . In this way, this measure allows us to evaluate the heterogeneity of the mortality levels among a set of populations. The specific case of a coherent multi-population model corresponds to a situation where for all $x \in \mathcal{X}$ the dispersion $(\delta_{x,t}^{\mathcal{I}})_{t \in \mathcal{T}}$ is controlled and can not diverge.

2.2 The Lee-Carter model

There is a broad variety of mortality models that have been introduced in the actuarial science and demography literature. In this paper, we choose to focus on the Lee-Carter model, which is one of the most used by practitioners. We first quickly recall the model using the previous notation and adopting a multi-population point of view. Thus, Lee and Carter (1992) propose to model the central death rates of the i -th population such as

$$\ln m_{x,t}^{(i)} = \alpha_x^{(i)} + \beta_x^{(i)} \kappa_t^{(i)} + \epsilon_{x,t}^{(i)}, \quad (2.3)$$

where $\alpha_x^{(i)}$ and $\beta_x^{(i)}$ are age-specific effect parameters, $\kappa_t^{(i)}$ represent the temporal mortality dynamics, and $\epsilon_{x,t}^{(i)}$ are residual terms. For the sake of the uniqueness of the solution, the usual constraints are imposed in the estimation process

$$\sum_{t \in \mathcal{T}} \kappa_t^{(i)} = 0 \text{ and } \sum_{x \in \mathcal{X}} \beta_x^{(i)} = 1. \quad (2.4)$$

Thus, $\alpha_x^{(i)}$ are set to be the averages of log mortality central rates over the period \mathcal{T} considered, and the series of parameters $\beta_x^{(i)}$ and $\kappa_t^{(i)}$ are estimated thanks to the application of the singular value decomposition (SVD) method.

Furthermore, we model the dynamic of the time series $\kappa_t^{(i)}$ as a random walk with a drift $c^{(i)}$

$$\kappa_t^{(i)} = c^{(i)} + \kappa_{t-1}^{(i)} + e_t^{(i)}, \quad (2.5)$$

where the innovations $(e_t^{(i)})_{i \in \mathcal{I}}$ is an I -dimensional Gaussian white noises with mean 0 and a diagonal variance-covariance matrix Σ_1 .

The Lee-Carter (LC) being a single population mortality model, we note that no relationships between the different populations are taken into account. As a consequence, the derived mortality forecasts are independent and can diverge. It creates a potentially large diversification effect on the projection of the longevity risk within a stochastic multi-population framework.

2.3 The coherent Li-Lee model

As an alternative, Li and Lee (2005) extend the Lee-Carter model to the multi-population scope by imposing a common trend $B_x^{\mathcal{I}} K_t^{\mathcal{I}}$ to the collection \mathcal{I} of considered populations, i.e.

$$\ln m_{x,t}^{(i)} = \alpha_x^{(i)} + B_x^{\mathcal{I}} K_t^{\mathcal{I}} + \beta_x^{(i)} \kappa_t^{(i)} + \epsilon_{x,t}^{(i)}. \quad (2.6)$$

The coherence is then enforced by modeling the dynamic of time series $\kappa_t^{(i)}$ via a mean-reverting process. We retain here a first order autoregressive (AR) model

$$\kappa_t^{(i)} = a^{(i)} \kappa_{t-1}^{(i)} + r_t^{(i)}, \quad (2.7)$$

where the innovations $(r_t^{(i)})_{i \in \mathcal{I}}$ are an I -dimensional Gaussian white noises with mean 0 and a diagonal variance-covariance matrix Σ_2 . We denote $m_{x,t}^{\mathcal{I}}$ the mortality rates of the overall population, i.e. the gathering of all populations from the collection \mathcal{I}

$$m_{x,t}^{\mathcal{I}} = \frac{D_{x,t}^{\mathcal{I}}}{E_{x,t}^{\mathcal{I}}}, \quad (2.8)$$

where $D_{x,t}^{\mathcal{I}} = \sum_{i \in \mathcal{I}} D_{x,t}^{(i)}$ and $E_{x,t}^{\mathcal{I}} = \sum_{i \in \mathcal{I}} E_{x,t}^{(i)}$. Thus, the fit of a Lee-Carter model on these series, under the usual constraints $\sum_{t \in \mathcal{T}} K_t^{\mathcal{I}} = 0$ and $\sum_{x \in \mathcal{X}} \beta_x^{\mathcal{I}} = 1$, gives the common trend factor estimates. Like in

the single population context, the age–population specific series of parameters $\alpha_x^{(i)}$ are set to be the averages of log-mortality central rates over the training period \mathcal{T} . Finally, the population–specific temporal dynamic factors $\beta_x^{(i)} \kappa_t^{(i)}$ are obtained thanks to the SVD method, with the constraints $\sum_{t \in \mathcal{T}} \kappa_t^{(i)} = 0$ and $\sum_{x \in \mathcal{X}} \beta_x^{(i)} = 1$, for each $i \in \mathcal{I}$.

Similarly to the Lee–Carter model, time series $K_t^{\mathcal{I}}$ is modeled as a random walk with drift

$$K_t^{\mathcal{I}} = c^{\mathcal{I}} + K_{t-1}^{\mathcal{I}} + e_t^{\mathcal{I}}, \quad (2.9)$$

where $e_t^{\mathcal{I}}$ is a Gaussian white noise with mean 0 and related variance $\sigma_{\mathcal{I}}^2$.

Thus defined, the Li–Lee (LL) extension enforces the specific mortality rates of the whole collection \mathcal{I} of populations to follow the same trend and converge in the long-run. Even if the population–specific temporal factors $\kappa_t^{(i)}$ allow a population to slightly deviate from this trend for a short period of time, the mean–reverting property brings it back to the common dynamic over the long run. From a longevity risk management point of view, it then implies a limited diversification among the population in a stochastic evaluation context.

2.4 Mortality dispersion on the HMD

Let us now focus on a group of 16 western European countries, namely: Austria (AUT), Belgium (BEL), Switzerland (CHE), West Germany (DEUW), Denmark (DNK), Spain (ESP), Finland (FIN), France (FRA), Ireland (IRL), Italy (ITA), Luxembourg (LUX), Netherlands (NLD), Norway (NOR), Portugal (PTR), Sweden (SWE) and Great Britain (GBR). Furthermore, we consider separately the male and female populations for each country. Thus, our collection \mathcal{I} of interest is composed of $I = 32$ populations, each one of them being defined by a couple (country, sex). The data is extracted from the Human Mortality Database (HMD, 2019). For the age–period training set, we retain $\mathcal{X} \times \mathcal{T} = \{45, \dots, 90\} \times \{1960, \dots, 2014\}$, and we fit single LC models as well as a LL model, as described in Sections 2.2 and 2.3. The Figure 1 represents the dispersion $\delta_{85,t}^{\mathcal{I}}$ estimated on the historical data and on the projections over 50 years obtained with the both stochastic mortality models. For the latter, we plot the median together with the 95% prediction intervals derived from 500 Monte-Carlo simulations.

First, let us remark that the dispersion measure at age 85 has nearly doubled between the 1960’s and the 2000’s, and seems more stable in recent years. As expected, the predicted dispersion is significantly different between the results from the LC and the LL models. In the first case, both the median and the width of the prediction intervals of the dispersion increase linearly with the projection horizon. In other words, the mortality rates at age 85 of the considered populations become more and more dissimilar in average, and this heterogeneity significantly varies from one stochastic scenario to another. On the contrary, the LL’s forecasts exhibit a strongly stable dispersion: according to them, not only the median is constant over time, but also the confidence intervals are very narrow comparing to the historical data and their bandwidth does not augment with the projection horizon. In term of generated mortality scenarios, it implies that a considerable majority of them lead to very similar pattern of mortality rates, even in the long term.

Both the LC and LL models present drawbacks when analyzing the projected dispersion in a longevity risk management framework. By not imposing any relationships between the population mortality dynamics, the LC model artificially creates some diversification in term of longevity risk. Contrariwise, the LL model imposes a strong coherence hypothesis on all the populations, thus leaving no significant scope for even a limited deviation of the mortality between the populations:

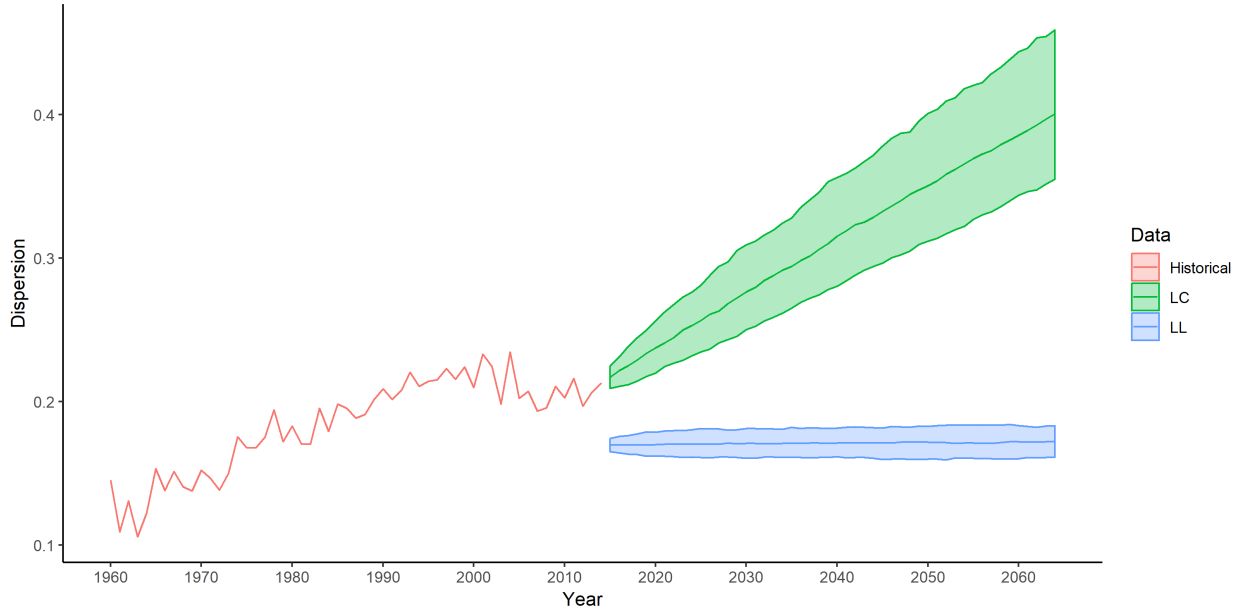


Figure 1: Dispersion at age 85 in the western European populations: historical data and median projections by Lee-Carter and Li-Lee models with the corresponding 95% prediction intervals.

it assumes a high concentration risk in the longevity evaluation. Intuitively, a longevity risk manager may want to consider some intermediate scenarios between the exaggerated LC’s diversification and LL’s over-concentration.

3 A locally coherent approach

To bridge the gap between the Lee-Carter’s diversification and the Li-Lee’s concentration, we propose a new model based on the idea that the populations are coherent by homogeneous groups, and not all together at the same time. In the populations space, it can be seen as a local version of the coherence property.

3.1 The model

Keeping the notation introduced before, we now denote \mathcal{J} a partition of the populations collection \mathcal{I} in J distinct groups. Let $\phi : \mathcal{I} \rightarrow \mathcal{J}$ be the corresponding classification function that labels a population to a specific group. We then propose the following model for each population $i \in \mathcal{I}$

$$\ln m_{x,t}^{(i)} = \alpha_x^{(i)} + B_x^{\phi(i)} K_t^{\phi(i)} + \mathbb{1}_{\{\#\phi(i) > 1\}} \beta_x^{(i)} \kappa_t^{(i)} + \epsilon_{x,t}^{(i)}, \quad (3.1)$$

where $\# : \mathcal{J} \rightarrow \mathbb{N}$ is the cardinal function of a group, and $\phi(i)$ denotes the coherence group of the population i .

Similarly to the LL model, for each group $j \in \mathcal{J}$, the local common trend factors B_x^j and K_t^j are estimated by fitting a Lee-Carter model thanks to the SVD method on the group log mortality rates data

$$m_{x,t}^j = \frac{D_{x,t}^j}{E_{x,t}^j}, \quad (3.2)$$

where $D_{x,t}^j = \sum_{i \in \mathcal{J}} D_{x,t}^{(i)}$ and $E_{x,t}^j = \sum_{i \in \mathcal{J}} E_{x,t}^{(i)}$, with the usual uniqueness constraints. For each population i , the series of age factors $\alpha_x^{(i)}$ are set to be the averages of log mortality rates over the estimation period \mathcal{T} . Finally, the population-specific mortality dynamic parameters $\beta_x^{(i)}$ and $\kappa_t^{(i)}$ are again estimated through SVD, if the considered population i is assumed to be coherent with at least one of the other population.

To impose the local coherence, we keep the AR(1) dynamic of Equation (2.7) for the population-specific period factors, but here we do not impose the variance-covariance matrix Σ_2 of the innovations $\left(r_t^{(i)}\right)_{i \in \mathcal{I}}$ to be diagonal anymore. This allows to capture short-term relationships between the populations.

Likewise, we also generalize the temporal dynamics of the period group factors to capture possible relationships between the different clusters of populations. Following the underlying idea of Kleinow (2015) and Zhou et al. (2014), we retain a vector autoregressive (VAR) model. For $j \in \mathcal{J}$, we note $\Delta K_t^j = K_t^j - K_{t-1}^j$ the common mortality improvement of the cluster. Given a temporal lag p , the dynamic of the VAR(p) is then given by

$$\Delta \mathbf{K}_t = \mathbf{C} + \sum_{k=1}^p \mathbf{A}_k \Delta \mathbf{K}_{t-k} + \mathbf{E}_t, \quad (3.3)$$

where $\Delta \mathbf{K}_t = \left(\Delta K_t^j\right)_{j \in \mathcal{J}}$ is the vector of mortality improvements at a group level, \mathbf{A}_k , $k = 1, \dots, p$, are $J \times J$ -autoregressive matrices, \mathbf{C} is a J -dimensional vector of drifts, and \mathbf{E}_t is a J -dimensional Gaussian white noise with mean 0 and Σ_1 the related covariance matrix. The matrices \mathbf{A}_k , $k = 1, \dots, p$, capture the long-run relationships of mortality improvements between groups of coherent populations, while the variance-covariance matrix Σ_1 estimates the short-term dependence structure of innovation shocks.

3.2 Border cases

Before continuing to the practical application of the model and its assessment, we focus on two special border cases. Indeed, by choosing some particular clusters and setting specific parameters, we note that our model includes the original Lee-Carter and Li-Lee models. To recover the LC model, we need to impose the following specifications:

- All the coherence clusters contain only one population, i.e. $\forall i \in \mathcal{I}, \phi(i) = \{i\}$. In other words we do not impose any coherence between the populations of interest.
- The temporal lag p of the VAR dynamic is set to 0. This point can also be approximated by applying a high λ in the elastic-net estimation process. The vector \mathbf{C} in Equation (3.3) is then equivalent to the concatenation of the population-specific drifts $c^{(i)}$ from Equation (2.5).
- A diagonal structure is enforced to the variance-covariance matrix Σ_1 , i.e. no short-term dependence structure is estimated between the populations.

Similarly, we can also retrieve the LL framework from our model by considering the following constraints.

- All the populations are grouping into a single cluster, i.e. $\forall i \in \mathcal{I}, \phi(i) = \mathcal{I}$, the coherence property is imposed to the whole demographic set.
- The temporal lag p of the VAR dynamic is set to 0. In particular, we remark that it is a 1-dimensional VAR due to the partition specification.
- A diagonal structure is enforced to the variance-covariance matrix Σ_2 . Further more, Σ_1 being a 1×1 -matrix, we recover the σ_7^2 of the LL's common temporal trend dynamic.

Hence, our model framework can be seen as a bridge between the Lee-Carter and the Li-Lee ones. Thereby, for the rest of this paper, we denote it by LC-LL.

3.3 VAR Elastic-Net

In a general context, one can consider a large number J of groups by assuming that the coherence hypothesis is too strong for the populations of interest, thereby increasing dramatically the number of parameters to be estimated in the VAR(p). From a statistic point of view, it may lead to high-dimensional problems with a limited number of observations. Following Guibert et al. (2019), we apply the extension of the elastic-net regularization and variable selection method proposed by Zou and Hastie (2005) for the high-dimensional estimation of our autoregressive matrices. This technique is a combination of the LASSO \mathcal{L}_1 -penalty, introduced by Tibshirani (1996), and the ridge \mathcal{L}_2 -penalty developed by Hoerl and Kennard (1970). Elastic-net has similar properties of variable selection as the LASSO. Moreover, it provides a grouping effect: highly correlated variables tend to be selected or dropped together. LASSO and elastic-net have already been extended to VAR model (Gefang, 2014; Basu et al., 2015), mostly with an economic application (see e.g. Song and Bickel, 2011; Furman, 2014) and more recently for mortality modelling (Guibert et al., 2019).

Therefore, we estimate the VAR(p) model presented in Equation (3.3) with T observations of the process $\Delta \mathbf{K}_t$ for $t \in \mathcal{T} = \{t_{\min}, \dots, t_{\max}\}$ by minimizing the criterion

$$L(\mathbf{C}, \mathbf{A}_1, \dots, \mathbf{A}_p) = \frac{1}{T-p} \sum_{t=t_{\min}+p}^{t_{\max}} \left\| \Delta \mathbf{K}_t - \mathbf{C} - \sum_{k=1}^p \mathbf{A}_k \Delta \mathbf{K}_{t-k} \right\|_2^2 - \alpha \lambda \sum_{k=1}^p \|\mathbf{A}_k\|_1 - \frac{(1-\alpha)\lambda}{2} \sum_{k=1}^p \|\mathbf{A}_k\|_2^2, \quad (3.4)$$

where $\|\cdot\|_1$ and $\|\cdot\|_2$ respectively denote the \mathcal{L}_1 and \mathcal{L}_2 norms, $\lambda > 0$ determines the strength of the penalization, and $\alpha \in [0, 1]$ represents the mix between ridge ($\alpha = 0$) and LASSO ($\alpha = 1$) penalties. In particular, when α is set such as some LASSO penalty is enforced, i.e. $\alpha > 0$, the higher λ gets, the fewer number of variables is selected.

For sparsity purpose we impose a larger weight to the LASSO penalty by setting α to 0.9. The hyper-parameter λ is then estimated thanks to a 10-folds cross-validation method. To apply this estimation process, we use the `sparsevar` R-package (Vazzoler et al., 2016), which is based on the `glmnet` one (Friedman et al., 2010). Furthermore, we choose to retain a temporal lag $p = 4$ in the rest of the paper.

4 Numerical applications

In this section, we compare the forecasting results with different locally coherent specifications for European populations introduced in Section 2.4. First, we investigate clustering strategies to determine the coherence groups among the collection of populations. We retain two approaches: expert-based and data-driven. Second, we focus on the main mortality trends that can be derived from these approaches, and their related stochastic scenarios spectrum. Finally, we illustrate the effect of the grouping assumptions on the solvency capital required of a pension product.

4.1 Population clustering

At first glance, the clustering methods can roughly be split between those based on expert judgments and those more data-driven. In the following, we give one example of each for the collection of western European countries studied in the Section 2.4. Our aim here is rather to give an outlook of some reasonable clustering alternatives than describing exhaustively a methodology for grouping populations. Indeed, such an analysis is a complex task and is out of the scope of this paper, since it requires to examine not only mortality data (Hatzopoulos and Haberman, 2013) but also economical, social and environmental criteria as well as the health system of each population.

4.1.1 Coherence by country

In our case, the set of countries we are focusing on tend to strengthen their gender policy in the future. Thus, in the long run, one can assume that within a single country both male and female populations would have similar lifestyle with access to the same level of education, wealthiness and healthcare, leaving mostly only biological differences. Thereby, we define the partition \mathcal{J}_{MF} such as it clusters the populations by countries. The number of groups J equals then to 16. The corresponding model is noted LC-LL(MF).

An interesting point of this approach is that the VAR model estimates a dependence structure between the countries, allowing a rather easy reading of the autoregressive matrices that represent the underlying dynamics. Indeed, the common period factors $(K_t^j, j \in \mathcal{J}_{MF})$ are equivalent to the ones obtained by fitting single population LC models on the overall country. We display the Granger causality matrices in Figures 8a to 8d of the Appendix 2.

4.1.2 A data mining approach

The main idea of the coherence in the Li-Lee model is to impose a common trend $(K_t^{\mathcal{I}})_{t \in \mathcal{T}}$ in the mortality dynamics of each population i . This is done by fitting a Lee-Carter on the overall population of the retained collection \mathcal{I} (see Section 2.3). Hence, for a single population i , we consider its time series $(\kappa_t^{(i)})_{t \in \mathcal{T}}$, derived from the LC fitting, as a signature of the mortality dynamics.

To determine the coherence groups, we then apply an unsupervised clustering method on these signatures. We choose the well-known hierarchical cluster analysis (HCA) method. In particular, we retain the Euclidean metric and Ward's criterion as dissimilarity measure and linkage criterion respectively. We display the corresponding dendrogram in Figure 2.

We remark that, unlike the previous clustering, the populations are not gathered by country. It even seems to be the opposite: the gender indicator is one of the major splitting criteria. Yet, we

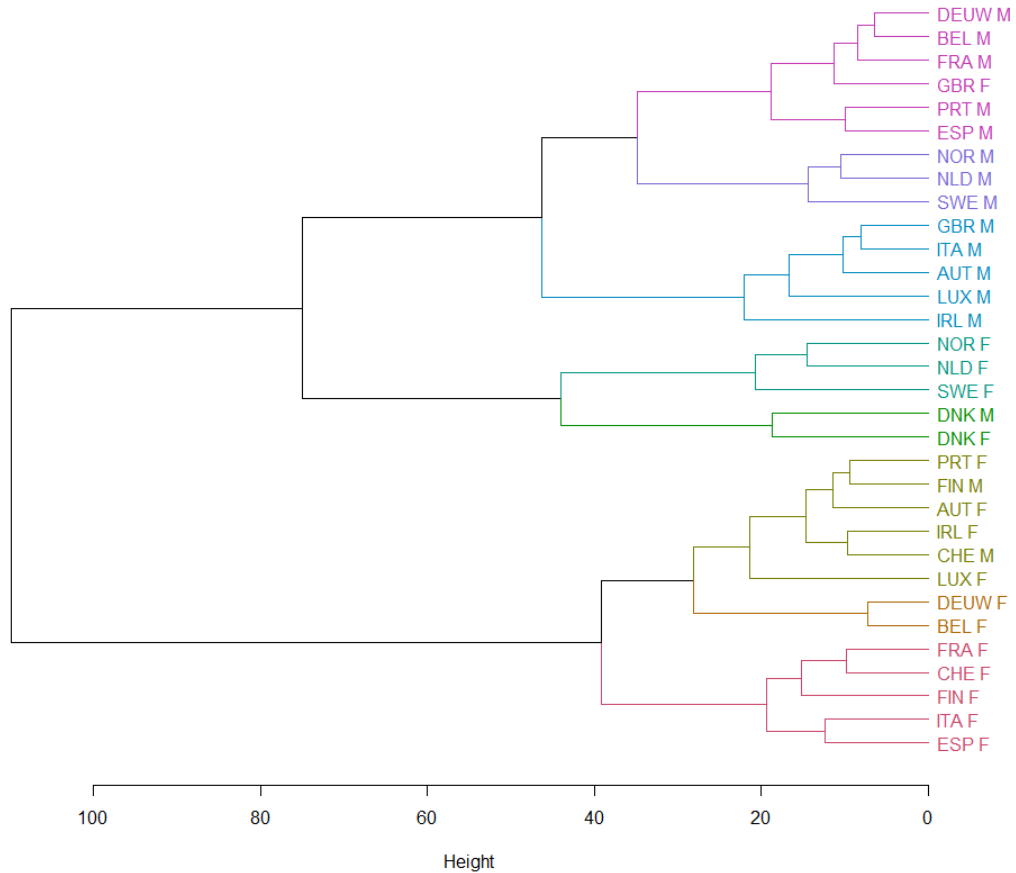


Figure 2: Dendrogram associated with the HCA applied on the LC's κ_t , colored according to 8 final clusters. The acronyms for countries are defined in Section 2.4; F and M represent female and male populations.

note one exception to this comment: the two Danish populations are clustered together, apart from other countries, suggesting that the Danish mortality dynamic exhibits some specific features when comparing to other western European countries.

For the following numerical applications, we choose to retain 8 different clusters, which are emphasized in the Figure 2 through the colors and recalled in the Table 1. We denote the LC-LL mortality model based on this clustering by LC-LL(HCA8), and the corresponding partition by $\mathcal{J}_{\text{HCA8}}$.

4.2 Dispersion forecasting

We now compare the models that we introduced, i.e. LC, LL, LC-LL(MF) and LC-LL(HCA8), in terms of dispersion. Rather than focusing on the main mortality trends that can be derived from these models, we are more interesting in the scope of this paper to the stochastic scenarios spectrum generated by these models.

Table 1: 8 groups of populations determined by HCA on the LC's κ_t .

Group 1	Group 2	Group 3	Group 4	Group 5	Group 6	Group 7	Group 8
DEUW M	NOR M	GBR M	NOR F	DNK M	PRT F	DEUW F	FRA F
BEL M	NLD M	ITA M	NLD F	DNK F	FIN M	BEL F	CHE F
FRA M	SWE M	AUT M	SWE F		AUT F		FIN F
GBR F		LUX M			IRL F		ITA F
PRT M		IRL M			CHE M		ESP F
ESP M					LUX F		

Following the Section 2.4, we display respectively in Figures 3 and 4 the projections obtained from the LC–LL(MF) and LC–LL(HCA8) approaches, compared to the LC and LL model forecasts. The red lines correspond to the historical dispersion $\delta_{85,t}^{\mathcal{I}}$ for the 32 European populations of \mathcal{I} at age 85. The same graphs are displayed in Appendix 1 for ages 70, 75, 80 and 90. As expected, the dispersion predictions produced by the LC–LL models are contained between the LC and LL ones.

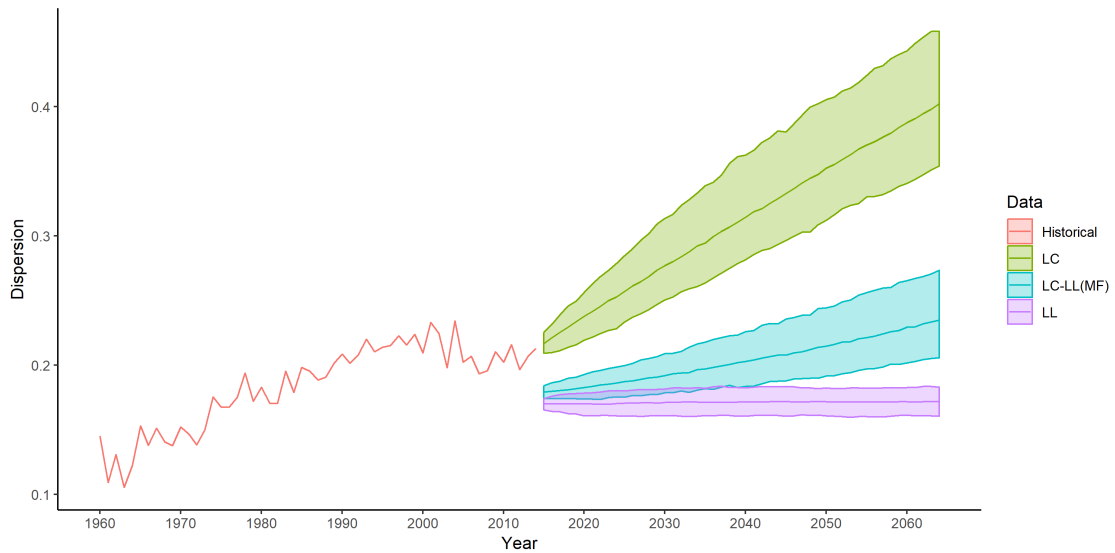


Figure 3: Dispersion at age 85 in the western European populations: historical data and median projections by LC, LL and LC–LL(MF) models with the corresponding confidence intervals at 5% and 95%.

In the LC–LL(MF) case, we note that the dispersion level is comparable to the LL’s projection during the first years, however both the mean dispersion and the width of the confidence intervals are increasing with the projection horizon like in the LC model. This increase is yet significantly slower than the one obtained with the single population framework. While the latter causes a doubling of the dispersion within 50 years, the LC–LL(MF) leads to a dispersion spectrum relatively close to the historical observations of this measure since the 1990’s.

When focusing on the LC–LL(HCA8), we observe that the dispersion dynamic is similar to the LC: both of the models leads to a significant augmentation of the dispersion compared to the historical data. However, in the multi-population model, the increases of the main trend and confidence intervals are more limited. In term of longevity risk, it leads to a significant lower diversification level among the populations.

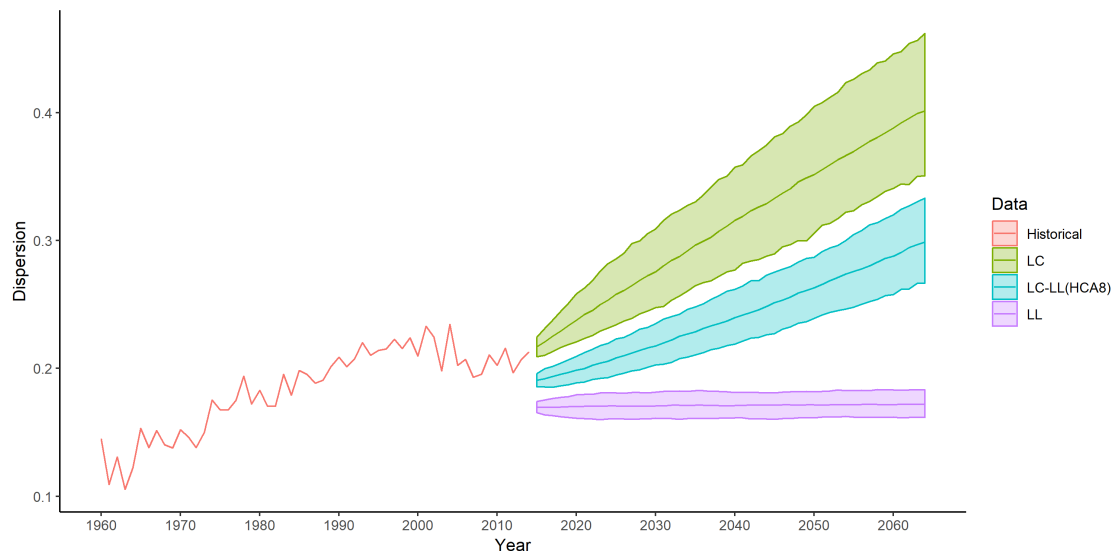


Figure 4: Dispersion at age 85 in the western European populations: historical data and median projections by LC, LL and LC-LL(HCA8) models with the corresponding confidence intervals at 5% and 95%.

4.3 Solvency Capital Requirement evaluation

Finally, we quantify the impact that the different models could have for a global (re)insurance company in terms of solvency capital requirement evaluation with respect to the longevity risk. To do so, we analyze a simplified situation where the liabilities are pensions to be paid between ages 60 to 90 for each of the 32 populations. Moreover, we focus only on the cohort aged 59 in 2014 and assume that at the valuation date, i.e. end of the year 2014, the number of pensioners is the same in every population. For the sake of simplicity, we retain an annual pension of 100 paid at the end of the year, and a constant discount rate of 1%.

Hence, to evaluate the corresponding provision the actuary needs to forecast the mortality rates $m_{59+t, 2014+t}^{(i)}$ for $(i, t) \in \mathcal{I} \times \{1, \dots, 32\}$. Following the Solvency II framework, the associated longevity risk solvency capital requirement (SCR) is obtained by estimating the Value at Risk (VaR) at a 99.5% level of the best estimate provision. This is done by simulating 2,000 longevity scenarios through the stochastic mortality models. We display in the Table 2 the results of this approach for the LC, LL, LC-LL(MF) and LC-LL(HCA8) models.

Table 2: Best estimate provision and Solvency capital requirement estimates.

	LC	LL	LC-LL(MF)	LC-LL(HCA8)
Provisions (mean)	67,513	67,577	67,675	67,485
VaR 99.5 %	68,059	69,591	68,999	68,954
SCR (VaR - mean)	547	2,014	1,323	1,469

First, we remark that the choice of the model, among the collection we explore in this paper, does not impact much the provision. The absolute difference between the highest provision estimate and the lowest one is of 190, which represents less than 0.3% of the latter. On the contrary, the

range of SCR is significantly wider. As expected, the LC leads to the lowest value because the mortality scenarios are independent from one population to another, thus creating diversification. In comparison, the SCR estimated by the LL is nearly 3.7 times bigger. Indeed, in this case the mortality rate dynamics of all populations follow the same trend, thereby implying a concentration risk on this trend. Finally, between these two extreme modelings, our locally coherent approach leads to intermediate levels of SCR. For the coherent groups determined in Section 4.1, we retrieve approximately the average between the LC and the LL results.

5 Toward a dynamic local coherence

In our model introduced in Section 3.1, we have supposed that the classification function $\phi : \mathcal{I} \rightarrow \mathcal{J}$ is constant through time. In other words, a population indefinitely belongs to the same group of coherence. However, in a more general longevity risk assessment framework, it could be interesting to study scenarios in which populations are allowed to switch from one coherence group to another. One of the motivations for such sensitivities is driven by the evaluation of basis risk in some longevity risk hedges. The aim of this section is to describe the stochastic forecasts of the mortality rates in a trend switching framework. Further, we highlight the effect of such switches on a Longevity Divergence Index Value (LDIV).

5.1 Trend switching model

Hereafter, the groups of local coherence $j \in \mathcal{J}$ are rather to be considered as dominant mortality trends which lead the mortality dynamics of their related specific populations. Thus, as long as a group of populations are lead by the same dominant trend, they are all coherent between them. On the contrary to the model of Section 3.1, we consider here that \mathcal{J} is not necessarily a partition of the retained collection of populations \mathcal{I} anymore. However, it can always be viewed as a partition of a larger collection of populations Ω , which is not fully observed. Thus, depending of the time period, some of the dominant trends $j \in \mathcal{J}$ may not be linked to any retained population $i \in \mathcal{I}$. During such periods, they can be viewed as dominant trends, exogenous from the observed collection of populations. In the same way, we can assume that $\forall j \in \mathcal{J}, \#j > 1$, even if it implies assuming the existence of populations in Ω which are not present in the retained collection of populations \mathcal{I} .

Thus, for $(i, x, t) \in \mathcal{I} \times \mathcal{X} \times \mathcal{T}$, we propose the following dynamics for the central mortality rates

$$\ln m_{x,t}^{(i)} = \alpha_x^{(i)} + B_x^{\phi_t(i)} K_t^{\phi_t(i)} + \beta_x^{(i)} \kappa_t^{(i)} + \text{ad}_{x,t}^{(i)} + \epsilon_{x,t}^{(i)}, \quad (5.1)$$

where function $\phi_t : \mathcal{I} \rightarrow \mathcal{J}$ return a set of classification functions, $\alpha_x^{(i)}$ are specific population mortality levels, (B_x^j, K_t^j) define the dominant mortality trends, $(\beta_x^{(i)}, \kappa_t^{(i)})$ represent specific population mortality dynamics, $\text{ad}_{t,x}^{(i)}$ are adjustment mortality levels. Considering the time series, we keep the dynamics of the previous model, i.e. $\Delta \mathbf{K}_t$ follows a VAR(p) model, see Equation (3.3), and $\kappa_t^{(i)}$ are driven by AR(1) models.

The fact that the classification function ϕ_t is now dynamic, it may happen that the switch from one dominant trend to another creates a significant leap in the mortality dynamics. Indeed, for two different dominant trends (j_1, j_2) and a couple age-period (x, t) , we do not impose the term $B_x^{j_2} K_t^{j_2} - B_x^{j_1} K_t^{j_1}$ to be limited since it describes the difference between two non-coherent mortality

dynamics. Thus, to avoid such jumps in the mortality level each time a population changes of dominant trend, we need to add adjustment mortality levels:

$$\text{ad}_{x,t}^{(i)} = \sum_{s=t_0+1}^t B_x^{\phi_{s-1}(i)} K_s^{\phi_{s-1}(i)} - B_x^{\phi_s(i)} K_s^{\phi_s(i)}, \quad (5.2)$$

where t_0 is a time such as $\text{ad}_{x,t_0}^{(i)} = 0$ for all ages $x \in \mathcal{X}$. In a practical point of view, $\phi_{t_0}(i)$ defines the initial dominant trend of the population i . Furthermore, we note that, in the non-switching model case, we have $\forall s \in \mathcal{T}$, $\phi_{s-1}(i) = \phi_s(i) = \phi(i)$, so $\forall t \in \mathcal{T}$, $\text{ad}_{x,t}^{(i)} = 0$. Hence, we retrieve the dynamics of the LC-LL with constant groups of coherence, see Equation (3.1).

5.2 European LDIV

As previously stated, this extension is motivated by the assessment of basis risk in longevity risk hedges. We choose to focus on one practical example: the Longevity Divergence Index Value (LDIV) on which the Swiss Re Kortis bond is defined (Hunt and Blake, 2015).

Issued in December 2010, the Kortis bond was designed to hedge the basis risk resulting from Swiss Re's "partial natural hedge" in longevity risk. Indeed, the reinsurer was globally exposed to

- mortality risk on the US male population aged between 55 and 65,
- longevity risk on the UK male population aged between 75 and 85.

Even though these two exposures create a natural longevity hedge, a significant basis risk remains between them two, especially if the mortality trends of the corresponding populations diverge. In our model, it would be implied by the fact that the two populations are not linked to the same dominant trend.

The payout of the Kortis bond is based on the level of the LDIV in 2016. To compute this value, we first need to observe the annualized mortality improvement of each population i

$$\text{Improvement}_n^{(i)}(x, t) = 1 - \left[\frac{m_{x,t}^{(i)}}{m_{x,t-n}^{(i)}} \right]^{\frac{1}{n}}, \quad (5.3)$$

where n is the averaging period of the bond, equals to 8 years in the Kortis bond's case. Then, an averaged improvement index is computed over the age classes exposed to the risk

$$\text{Index}(t, i) = \frac{1}{1 + x_2^{(i)} - x_1^{(i)}} \sum_{x=x_1^{(i)}}^{x_2^{(i)}} \text{Improvement}_n^{(i)}(x, t), \quad (5.4)$$

where for the Kortis bond the age classes are $(x_1^{(\text{UK})}, x_2^{(\text{UK})}) = (75, 85)$ and $(x_1^{(\text{US})}, x_2^{(\text{US})}) = (55, 65)$. Finally, the LDIV at time t is obtained by

$$\text{LDIV}(t) = \text{Index}(t, i_1) - \text{Index}(t, i_2), \quad (5.5)$$

where in the Swiss Re case $(i_1, i_2) = (\text{UK}, \text{US})$ and $t = 2016$.

To illustrate the impact on the basis risk of a switch of dominant trend, we construct an European LDIV for:

- the Swiss female population, aged between 75 and 85, as the longevity risk exposure i_1 ;
- the French female population, aged between 55 and 65, as the mortality risk exposure i_2 ;
- a risk period n of 8 years, which ends at year $t = 2024$.

Moreover, we suppose that at $t_0 = 2014$, the mortality dynamics of the collection of populations \mathcal{I} follow the model of Section 4.1.2, i.e. the LC-LL(HCA8). Thus, the classification function ϕ_{t_0} can be described thanks to Table 1. Finally, we suppose that at a time $T > t_0$, the French female population switches from its original dominant trend to the dominant trend that the Belgian and German female populations are initially linked to. No further switch are considered. Hence, for $t > t_0$, we have

$$\phi_t(i) = \begin{cases} \phi_{t_0}(i) & \text{if } i \neq \text{FRA F} , \\ \phi_{t_0}(\text{FRA F}) & \text{if } i = \text{FRA F} \text{ and } t < T, \\ \phi_{t_0}(\text{BEL F}) & \text{if } i = \text{FRA F} \text{ and } t \geq T. \end{cases} \quad (5.6)$$

Figure 5 displays the sensibility of our European LDIV(2024) to the switching time T between $t_0 = 2016$ and 2024. To obtain the results, we simulate 10,000 stochastic mortality scenarios thanks to our model for each switching time between 2016, i.e. the start of the risk period and 2024, i.e. the end of the risk period. We then retain the median scenario in term of LDIV(2024). As expected, the sooner the switch occurs, the more significant the Longevity Divergence Index Value is. In particular, we remark that the LDIV is 1.8 times higher when the switch happens in 2016 than in 2024. Indeed, the longer the French and Swiss female populations are linked to different dominant trends, i.e. the longer they are not coherent, the more they diverge.

Thus, our extended model allows the longevity risk manager to evaluate the impact of a wide spectrum of stochastic longevity scenarios on his portfolio and the potential hedges together with the corresponding basis risks. In a context where basis risk is one the main challenges that the longevity risk transfer market is facing (Blake et al., 2019), our framework provides an innovative point of view for its assessment.

6 Conclusions

In this paper we propose a new notion for multiple populations mortality forecasting that we have named local coherence. Indeed, we remark that full independence and "full" coherence approaches both suffer from drawbacks when considering the mortality projections of a large set of populations. To highlight this point, we compare the dispersion over 32 European populations of mortality rate forecasts derived from Lee and Carter (1992) and Li and Lee (2005) models. In the first case, the diversification in the stochastic scenarios is overestimated, whereas, in the second method, the concentration is exaggerated.

To overcome this issue, our locally coherent mortality model allows to forecast populations with homogeneous mortality profiles by coherence groups, where the long-term relationships between inter-group populations are only modeled through a VAR process without any coherence constraints. Thus, it offers a trade-off between the two border coherence cases, which are included in our model. The practitioners have then the possibility to easily simulate a larger spectrum of longevity scenarios to evaluate their risks compared to the usual models cited before.

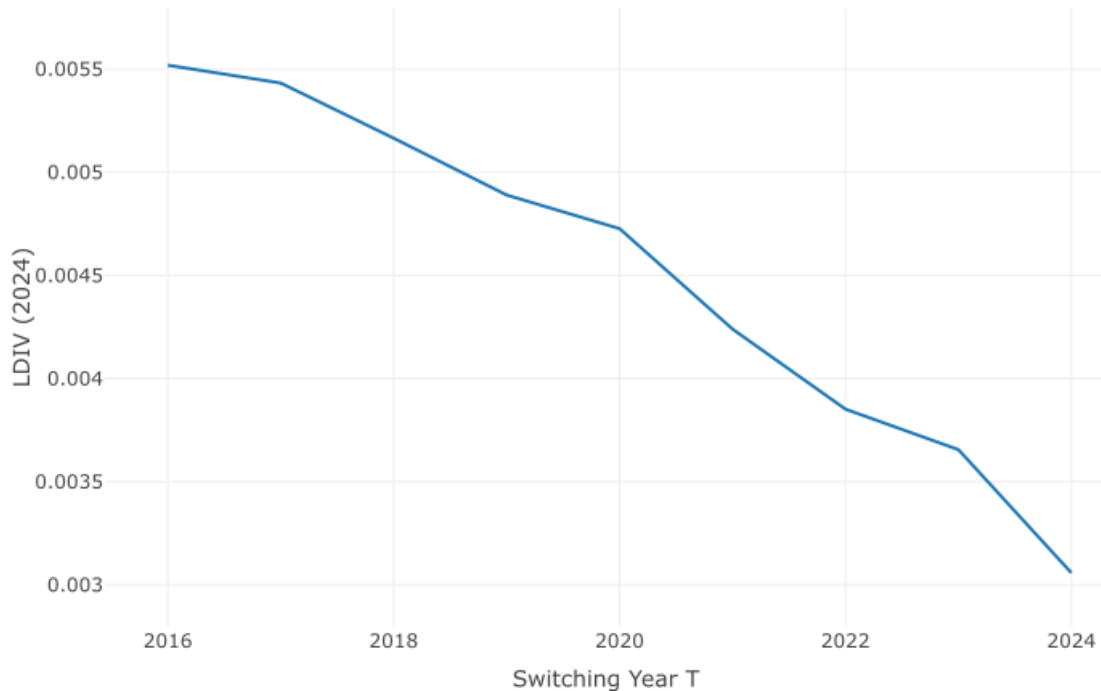


Figure 5: Median European LDIV(2024) according to the switching time of the French female population.

To assess the behavior of our model, we have compared it with the Lee-Carter and Li-Lee's ones over the set of European countries for some numerical applications. We notably show that the retained coherence hypothesis can have a major impact on the longevity risk solvency capital requirement for a global life insurance company within the Solvency II framework. Thereby, the large freedom of our model allows to evaluate more precisely this crucial risk measure.

Finally, we have extended the locality coherence property of our model to the temporal dimension. By allowing populations to switch from one group of coherence to another, we expand the spectrum of possible stochastic mortality scenarios. This innovative methodology is particularly interesting in a longevity hedges' basis risk assessment context. Thus, we propose a new framework that should be useful for the development of the longevity risk transfer market.

Our proposed method is a first step for modeling together both homogeneous and heterogeneous populations in terms of mortality profiles. It opens up some pathways for future research. We do not further investigate the difficult issue of how grouping a large set of populations. Our approach however stresses the importance of developing techniques for identifying homogeneous/heterogeneous groups of population based not only on trend and volatility patterns in mortality dynamics, but also by considering economical, social and environmental criteria or the effectiveness of the health system. In addition, we also believe that groups of populations evolve dynamically. This means that some groups have a behavior which gradually converge to those of another groups, e.g. the less developed countries would probably follow the trend of developed countries (Li et al., 2018), or diverge from each other. Another potential improvement is thus to consider methods for detecting change in the mortality trend, see e.g. El Karoui et al. (2017).

References

- Basu, S., Michailidis, G., and others (2015). Regularized estimation in sparse high-dimensional time series models. *The Annals of Statistics* 43.4, pp. 1535–1567. DOI: [10.1214/15-AOS1315](https://doi.org/10.1214/15-AOS1315).
- Bergeron-Boucher, M.-P., Simonacci, V., Oeppen, J., and Gallo, M. (2018). Coherent Modeling and Forecasting of Mortality Patterns for Subpopulations Using Multiway Analysis of Compositions: An Application to Canadian Provinces and Territories. *North American Actuarial Journal* 22.1, pp. 92–118. DOI: [10.1080/10920277.2017.1377620](https://doi.org/10.1080/10920277.2017.1377620).
- Blake, D., Cairns, A. J. G., Dowd, K., and Kessler, A. R. (2019). Still living with mortality: the longevity risk transfer market after one decade. *British Actuarial Journal* 24. DOI: [10.1017/S1357321718000314](https://doi.org/10.1017/S1357321718000314).
- Cairns, A. J. G., Blake, D., and Dowd, K. (2006). A Two-Factor Model for Stochastic Mortality with Parameter Uncertainty: Theory and Calibration. *Journal of Risk and Insurance* 73.4, pp. 687–718. DOI: [10.1111/j.1539-6975.2006.00195.x](https://doi.org/10.1111/j.1539-6975.2006.00195.x).
- Cairns, A. J. G., Kallestrup-Lamb, M., Rosenskjold, C., Blake, D., and Dowd, K. (2019). Modelling Socio-Economic Differences in Mortality Using a New Affluence Index. *ASTIN Bulletin: The Journal of the IAA* 49.3, pp. 555–590. DOI: [10.1017/asb.2019.14](https://doi.org/10.1017/asb.2019.14).
- Danesi, I. L., Haberman, S., and Millossovich, P. (2015). Forecasting mortality in subpopulations using Lee–Carter type models: A comparison. *Insurance: Mathematics and Economics* 62, pp. 151–161. DOI: [10.1016/j.insmatheco.2015.03.010](https://doi.org/10.1016/j.insmatheco.2015.03.010).
- Dowd, K., Cairns, A. J. G., Blake, D., Coughlan, G. D., and Khalaf-Allah, M. (2011). A Gravity Model of Mortality Rates for Two Related Populations. *North American Actuarial Journal* 15.2, pp. 334–356. DOI: [10.1080/10920277.2011.10597624](https://doi.org/10.1080/10920277.2011.10597624).
- El Karoui, N., Loisel, S., and Salhi, Y. (2017). Minimax optimality in robust detection of a disorder time in doubly-stochastic Poisson processes. *The Annals of Applied Probability* 27.4, pp. 2515–2538. DOI: [10.1214/16-AAP1266](https://doi.org/10.1214/16-AAP1266).
- Enchev, V., Kleinow, T., and Cairns, A. J. G. (2017). Multi-population mortality models: fitting, forecasting and comparisons. *Scandinavian Actuarial Journal* 2017.4, pp. 319–342. DOI: [10.1080/03461238.2015.1133450](https://doi.org/10.1080/03461238.2015.1133450).
- Friedman, J., Hastie, T., and Tibshirani, R. (2010). Regularization Paths for Generalized Linear Models via Coordinate Descent. *Journal of Statistical Software* 33.1, pp. 1–22.
- Furman, Y. (2014). VAR Estimation with the Adaptive Elastic Net. SSRN Scholarly Paper ID 2456510. Rochester, NY: Social Science Research Network.
- Gefang, D. (2014). Bayesian doubly adaptive elastic-net Lasso for VAR shrinkage. *International Journal of Forecasting* 30.1, pp. 1–11. DOI: [10.1016/j.ijforecast.2013.04.004](https://doi.org/10.1016/j.ijforecast.2013.04.004).
- Guibert, Q., Lopez, O., and Piette, P. (2019). Forecasting mortality rate improvements with a high-dimensional VAR. *Insurance: Mathematics and Economics* 88, pp. 255–272. DOI: [10.1016/j.insmatheco.2019.07.004](https://doi.org/10.1016/j.insmatheco.2019.07.004).
- Hatzopoulos, P. and Haberman, S. (2013). Common mortality modeling and coherent forecasts. An empirical analysis of worldwide mortality data. *Insurance: Mathematics and Economics* 52.2, pp. 320–337. DOI: [10.1016/j.insmatheco.2012.12.009](https://doi.org/10.1016/j.insmatheco.2012.12.009).
- HMD (2019). Human Mortality Database. University of California, Berkeley (USA), and Max Planck Institute for Demographic Research (Germany). Available at www.mortality.org (data downloaded on 2019-07-08).
- Hoerl, A. E. and Kennard, R. W. (1970). Ridge regression: Biased estimation for nonorthogonal problems. *Technometrics* 12.1, pp. 55–67. DOI: [10.1080/00401706.1970.10488634](https://doi.org/10.1080/00401706.1970.10488634).
- Hunt, A. and Blake, D. (2015). Modelling longevity bonds: Analysing the Swiss Re Kortis bond. *Insurance: Mathematics and Economics*. Special Issue: Longevity Nine - the Ninth International

- Longevity Risk and Capital Markets Solutions Conference 63, pp. 12–29. DOI: [10.1016/j.insmatheco.2015.03.017](https://doi.org/10.1016/j.insmatheco.2015.03.017).
- Kleinow, T. (2015). A common age effect model for the mortality of multiple populations. *Insurance: Mathematics and Economics*. Special Issue: Longevity Nine - the Ninth International Longevity Risk and Capital Markets Solutions Conference 63, pp. 147–152. DOI: [10.1016/j.insmatheco.2015.03.023](https://doi.org/10.1016/j.insmatheco.2015.03.023).
- Lee, R. D. and Carter, L. R. (1992). Modeling and Forecasting U. S. Mortality. *Journal of the American Statistical Association* 87.419, pp. 659–671. DOI: [10.2307/2290201](https://doi.org/10.2307/2290201).
- Li, H., Lu, Y., and Lyu, P. (2018). Coherent Mortality Forecasting for Less Developed Countries. SSRN Scholarly Paper ID 3209392. Rochester, NY: Social Science Research Network.
- Li, J. S.-H., Chan, W.-S., and Zhou, R. (2017). Semicoherent Multipopulation Mortality Modeling: The Impact on Longevity Risk Securitization. *Journal of Risk and Insurance* 84.3, pp. 1025–1065. DOI: [10.1111/jori.12135](https://doi.org/10.1111/jori.12135).
- Li, N. and Lee, R. (2005). Coherent mortality forecasts for a group of populations: An extension of the Lee-Carter method. *Demography* 42.3, pp. 575–594. DOI: [10.1353/dem.2005.0021](https://doi.org/10.1353/dem.2005.0021).
- Richman, R. and Wuthrich, M. V. (2018). A Neural Network Extension of the Lee-Carter Model to Multiple Populations. SSRN Scholarly Paper ID 3270877. Rochester, NY: Social Science Research Network.
- Song, S. and Bickel, P. J. (2011). Large vector auto regressions. arXiv preprint arXiv:1106.3915. University of California, Berkeley.
- Tibshirani, R. (1996). Regression shrinkage and selection via the lasso. *Journal of the Royal Statistical Society. Series B (Methodological)* 58.1, pp. 267–288. DOI: [10.1111/j.2517-6161.1996.tb02080.x](https://doi.org/10.1111/j.2517-6161.1996.tb02080.x).
- Vazzoler, S., Frattarolo, L., and Billio, M. (2016). sparsevar: A Package for Sparse VAR/VECM Estimation. R package version 0.0.10.
- Villegas, A. M., Haberman, S., Kaishev, V. K., and Millossovich, P. (2017). A comparative study of two-population models for the assessment of basis risk in longevity hedges. *ASTIN Bulletin: The Journal of the IAA* 47.3, pp. 631–679. DOI: [10.1017/asb.2017.18](https://doi.org/10.1017/asb.2017.18).
- Yang, S. S., Yeh, Y.-Y., Yue, J. C., and Huang, H. C. (2019). Understanding Patterns of Mortality Homogeneity and Heterogeneity Across Countries and Their Role in Modeling Mortality Dynamics and Hedging Longevity Risk. *North American Actuarial Journal*, pp. 1–24. DOI: [10.1080/10920277.2019.1662315](https://doi.org/10.1080/10920277.2019.1662315).
- Zhou, R., Wang, Y., Kaufhold, K., Li, J. S.-H., and Tan, K. S. (2014). Modeling Period Effects in Multi-Population Mortality Models: Applications to Solvency II. *North American Actuarial Journal* 18.1, pp. 150–167. DOI: [10.1080/10920277.2013.872553](https://doi.org/10.1080/10920277.2013.872553).
- Zhou, R., Xing, G., and Ji, M. (2019). Changes of Relation in Multi-Population Mortality Dependence: An Application of Threshold VECM. *Risks* 7.1, p. 14. DOI: [10.3390/risks7010014](https://doi.org/10.3390/risks7010014).
- Zou, H. and Hastie, T. (2005). Regularization and variable selection via the elastic net. *Journal of the Royal Statistical Society: Series B (Statistical Methodology)* 67.2, pp. 301–320. DOI: [10.1111/j.1467-9868.2005.00503.x](https://doi.org/10.1111/j.1467-9868.2005.00503.x).

Appendix 1 Dispersion projections

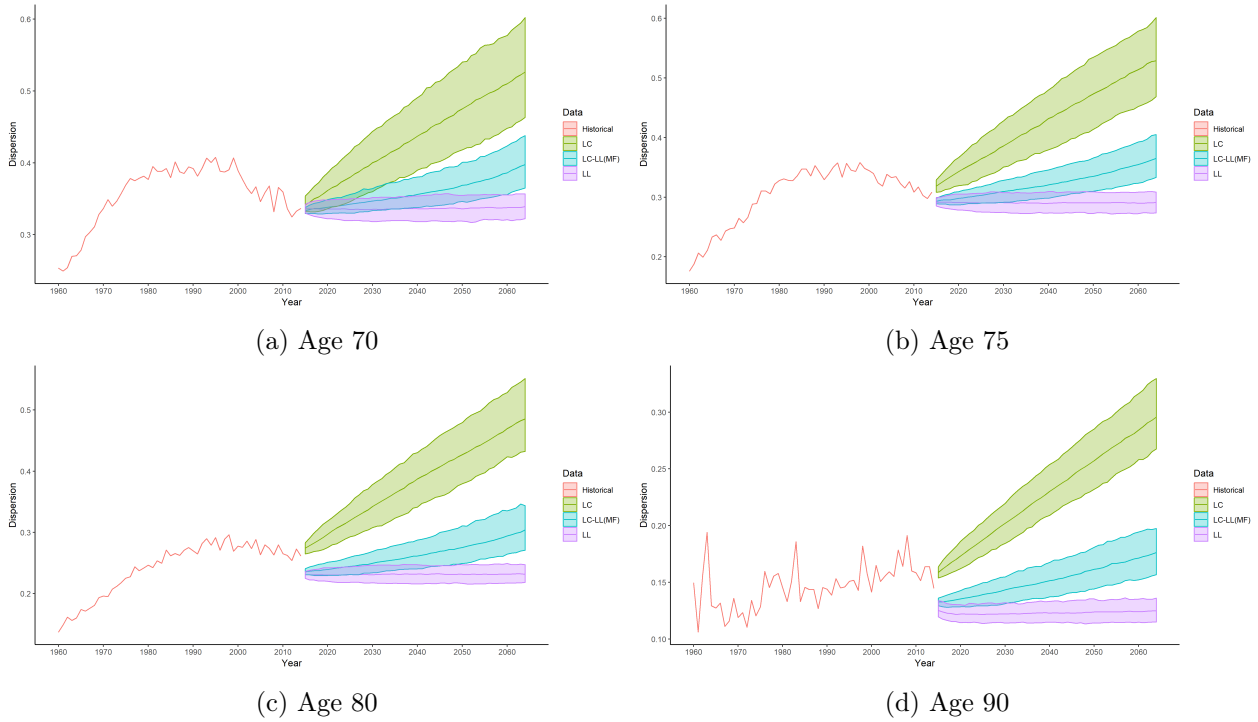
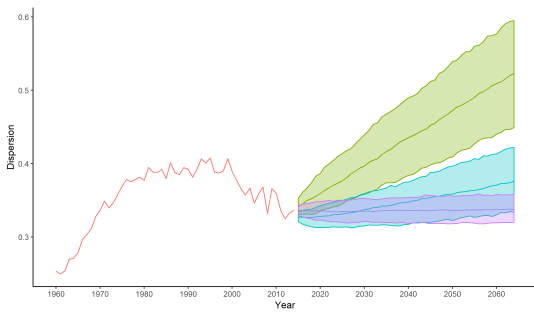


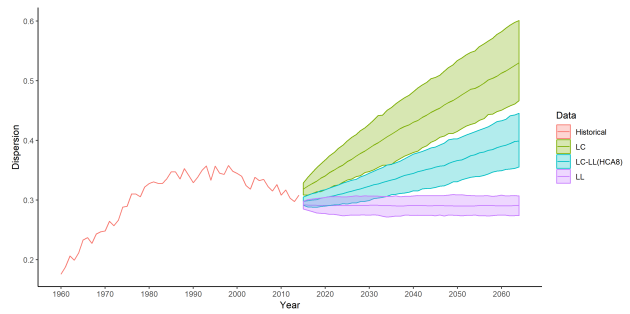
Figure 6: Dispersion in the western European populations: historical data and median projections by LC, LL and LC–LL(MF) models with the corresponding confidence intervals at 5% and 95%.

Appendix 2 Granger matrices from the LC-LL(MF) model

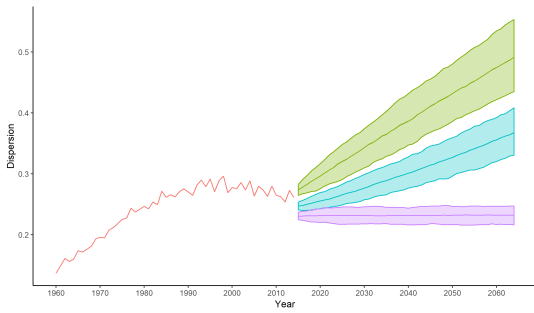
The matrix \mathbf{A}_1 (Figure 8a) exhibits mostly negative coefficients, shaped into a diagonal structure. We hereby capture the country-specific period effect. Indeed, when modeling the single population LC's $\kappa_t^{(i)}$ dynamics by an AR(1), we generally obtain negative autoregressive estimates. Displayed in a matrix way for a multi-population point of view, it leads to a negative diagonal matrix. We also remark some vertical patterns within the Granger causality matrices. In term of mortality dynamics, this should be interpreted as a persistent effect of a single country to a group countries. For example, in the autoregressive matrix \mathbf{A}_3 (Figure 8c), we note the existence of a positive vertical structure on the Swiss population. Hence, the Swiss mortality improvement seems to Granger cause the mortality improvement on 6 other countries, namely BEL, DEUW, GBR, IRL, NLD and PRT. A chock in the mortality rates in the Switzerland would then reverberate 3 years later in the 6 countries. In this way, the vertical structure can be seen as some kind of leader effect.



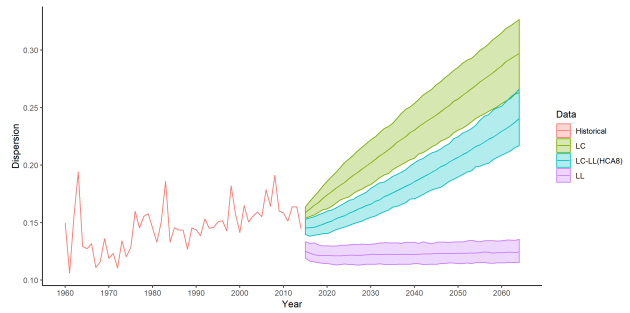
(a) Age 70



(b) Age 75



(c) Age 80



(d) Age 90

Figure 7: Dispersion in the western European populations: historical data and median projections by LC, LL and LC-LL(HCA8) models with the corresponding confidence intervals at 5% and 95%.

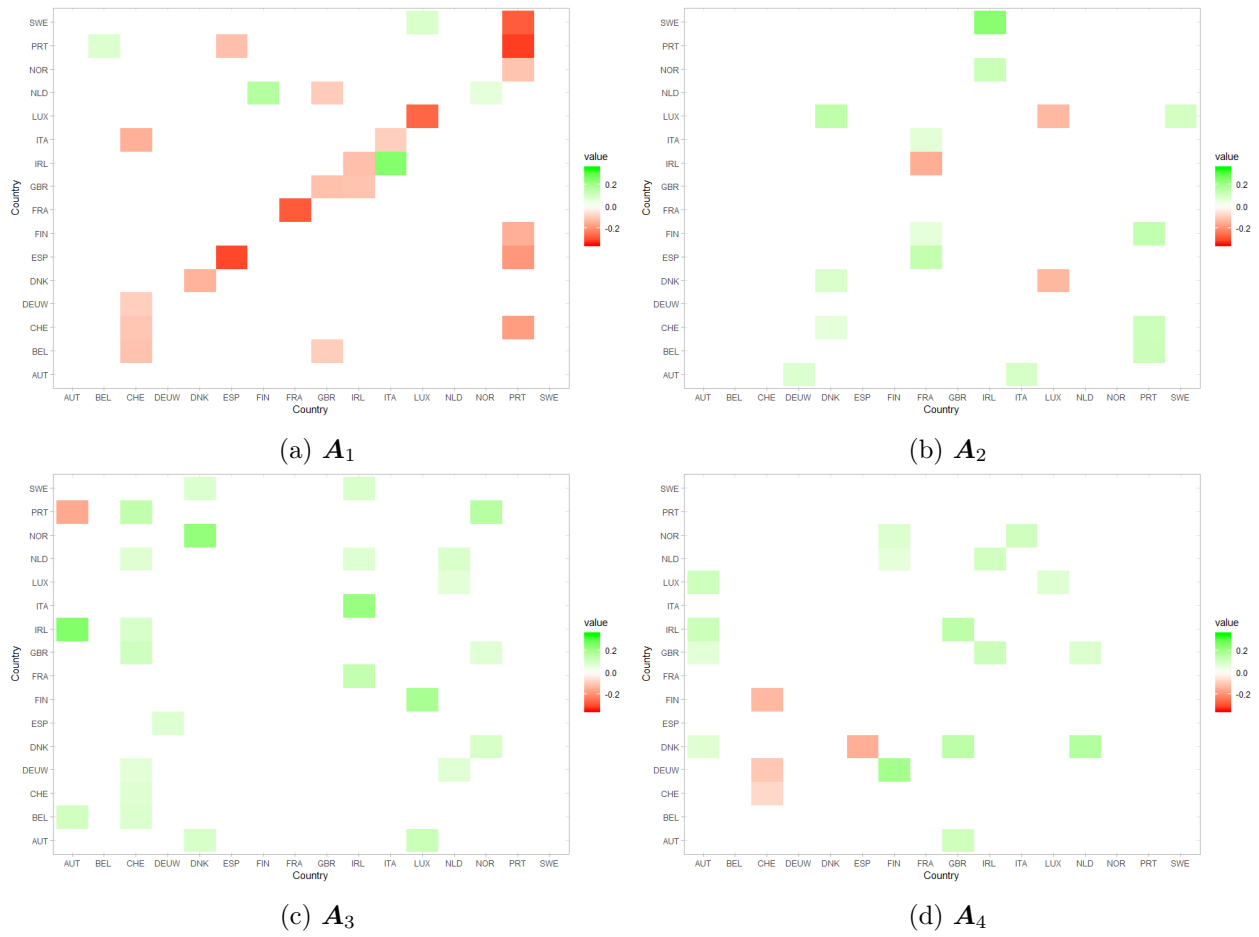


Figure 8: Estimated autoregressive matrices $\mathbf{A}_1, \dots, \mathbf{A}_4$ of the VAR-ENET from the LC-LL(MF) model.